CD13-positive bone marrow-derived myeloid cells promote angiogenesis, tumor growth, and metastasis

Eleonora Dondossola[a], Roberto Rangel[a,b], Liliana Guzman-Rojas[a,b], Elena M. Barbu[a], Hitomi Hosoya[a,c], Lisa S. St. John[d], Jeffrey J. Molldrem[d], Angelo Corti[e], Richard L. Sidman[f,g,1], Wadih Arap[a,1,2,3], and Renata Pasqualini[a,1,2,3]

[a]David H. Koch Center, The University of Texas MD Anderson Cancer Center, Houston, TX 77030; [b]Cancer Research Program, The Methodist Hospital Research Institute, Houston, TX 77030; [c]The US Naval Hospital Yokosuka, Fleet Post Office, AP, 96350-1600; [d]Department of Stem Cell Transplantation and Cellular Therapy, The University of Texas MD Anderson Cancer Center, Houston, TX 77030; [e]Division of Molecular Oncology, San Raffaele Scientific Institute, 20132 Milan, Italy; [f]Harvard Medical School, Boston, MA 02215; and [g]Department of Neurology, Beth Israel-Deaconess Medical Center, Boston, MA 02215

Contributed by Richard L. Sidman, November 9, 2013 (sent for review June 13, 2013)

Angiogenesis is fundamental to tumorigenesis and an attractive target for therapeutic intervention against cancer. We have recently demonstrated that CD13 (aminopeptidase N) expressed by nonmalignant host cells of unspecified types regulate tumor blood vessel development. Here, we compare CD13 wild-type and null bone marrow-transplanted tumor-bearing mice to show that host $CD13^+$ bone marrow-derived cells promote cancer progression via their effect on angiogenesis. Furthermore, we have identified $CD11b^+CD13^+$ myeloid cells as the immune subpopulation directly regulating tumor blood vessel development. Finally, we show that these cells are specifically localized within the tumor microenvironment and produce proangiogenic soluble factors. Thus, $CD11b^+CD13^+$ myeloid cells constitute a population of bone marrow-derived cells that promote tumor progression and metastasis and are potential candidates for the development of targeted antiangiogenic drugs.

mouse models | protease | stromal cells | vascular pericytes

Angiogenesis is a rate-limiting step in the development of many solid tumors, making it an attractive target for therapeutic intervention (1). Although pharmacologic modulation of angiogenesis has shown some clinical success, negative factors such as treatment-related plasticity, drug resistance, and tumor diversity have underscored the need for a better understanding of tumor-associated blood vessel formation at a mechanistic level (2). Tumor angiogenesis is a multifactorial process involving several different cell subtypes, especially tumor stromal endothelial cells, pericytes, carcinoma-associated fibroblasts (CAFs), and bone marrow-derived cells (BMDCs) (3, 4). A variety of immune cells directly support angiogenesis, including mast cells, tumor-associated macrophages (TAMs), and Tie2-expressing macrophages (TEMs) (5–7). Endothelial cells recruit inflammatory cells to the extravascular tissue by the expression of different leukocyte adhesion molecules. In turn, immune cells produce soluble factors, such as chemokines, cytokines, and proteases, that influence endothelial cell function and angiogenesis in a paracrine fashion (5). Other studies have shown that BMDCs have the ability to differentiate into endothelial cells, possibly by conversion first to endothelial progenitors (8–10).

Proteases activate growth factors and inhibit suppressive factors within tumors and are central to the angiogenic process within the tumor microenvironment (11). Studies on the involvement of aminopeptidases in tumor progression and angiogenesis have revealed a role for aminopeptidase N (CD13) expressed by stromal cells (12). Originally identified as a surface marker on myeloid cells (13), CD13 is a widely expressed membrane-bound metalloprotease involved in pleiotropic functions, including enzymatic cleavage of peptides, antigen presentation, and signal transduction that ultimately mediate downstream biological phenomena such as cell adhesion, proliferation, and motility (14). Diverse cell subpopulations (e.g., fibroblasts, pericytes, epithelial cells, tumor-initiating cells, and stem cells) express CD13 (15-19). Our group has shown that CD13 is a functional biomarker of angiogenesis (20) and is also expressed by tumor-associated blood vessels (21). Furthermore, by using CD13-null neonatal mice, we demonstrated an impaired angiogenic response in the oxygen-induced retinopathy-of-prematurity model, which quantifies retinal pathological neovascularization in response to hypoxia (22). We have also shown that CD13-null mice displayed dose-dependent reduced tumor growth after implantation with either B16-F10 melanoma or Lewis lung carcinoma (LLC) cells, largely because of impaired angiogenesis (12). These data indicate that CD13 expressed by host stromal cells mediates a pathological angiogenic response, but the specific cell subtypes involved in this phenomenon have yet to be identified.

Here, we unravel the type and role of $CD13^+$ stromal cells in tumor progression. By using CD13 wild-type (WT) and null (KO) mice in the setting of paired bone marrow transplantations, we demonstrate that $CD13^+$ BMDCs affect the progression of LLC, B16-F10 melanoma, and TSA mammary adenocarcinoma via their regulation of tumor angiogenesis. Notably, we show direct involvement of a $CD11b^+CD13^+$ myeloid subset of BMDCs in this process. Finally, we show that these cells produce angiogenic factors and specifically localize within the tumor microenvironment. Our results indicate that $CD11b^+CD13^+$ cells represent a population of proangiogenic BMDCs and that CD13 is crucial for their activity.

Significance

The progression of many solid tumors is associated with increased vascularization. We previously recognized involvement in tumor development and angiogenesis of tumor stromal cells expressing the CD13 protease aminopeptidase. The basic biological concept of participation of nontumor cells in the cancer stroma microenvironment is strengthened in the present study by our finding that a $CD11b^+CD13^+$ myeloid subset of bone marrow-derived cells affects pericyte biology and angiogenesis and thereby influences tumor growth and metastasis. Therapeutic implications of the identification of specific $CD11^+CD13^+$ myeloid bone marrow-derived cells as participants in the mechanism of tumor angiogenesis merit further investigation.

Author contributions: E.D., R.R., L.G.-R., R.L.S., W.A., and R.P. designed research; E.D., R.R., L.G.-R., E.M.B., H.H., and L.S.S.J. performed research; E.D., R.R., L.G.-R., L.S.S.J., J.J.M., A.C., R.L.S., W.A., and R.P. analyzed data; and E.D., A.C., R.L.S., W.A., and R.P. wrote the paper.

The authors declare no conflict of interest.

[1]To whom correspondence may be addressed. E-mail: richard_sidman@hms.harvard.edu, warap@salud.unm.edu, or rpasqual@salud.unm.edu.

[2]W.A. and R.P. contributed equally to this work.

[3]Present address: Department of Internal Medicine, The University of New Mexico Cancer Center, Albuquerque, NM 87106.

This article contains supporting information online at www.pnas.org/lookup/suppl/doi:10.1073/pnas.1321139110/-/DCSupplemental.

Results

In Vivo Characterization of CD13-Expressing Tumor Stromal Cells. Previous molecular and cellular analysis of LLC and B16-F10 melanoma tumor growth in CD13-null mice revealed that CD13 expression on nonmalignant host cells mediates tumor growth and angiogenesis (12). Given that endothelial cells, fibroblasts, pericytes, and immune cells (in particular, myeloid cells) display CD13 (13, 18, 19, 21), but no comprehensive studies on CD13 expression by tumor stromal cells have been performed, we first used FACS to quantitatively analyze LLC-, B16-F10–, and TSA-derived endothelial cells ($CD31^+$), pericytes/CAFs [α smooth muscle actin ($\alpha SMA)^+$] (23), myeloid cells ($CD45^+CD11b^+$), and other immune cells ($CD45^+CD11b^-$). Myeloid cells were the most frequent stromal cell population in the three tumor models studied (Fig. 1*A*). The majority of pericytes/CAFs (82–94%) expressed CD13, whereas about 40% of myeloid cells and 20% of endothelial cells expressed CD13 in all tumor models. Only a small subset of nonmyeloid immune cells expressed CD13 (Fig. 1*B*). Finally, we analyzed the cell surface expression among CD13-expressing stromal cell components within the tumor microenvironment. Myeloid cells represented 50–72% of CD13-expressing cells in all of the models analyzed, whereas endothelial cells varied between 6% and 30%, pericytes/CAFs were ∼10%, and other inflammatory cells were ∼3–9% (Fig. 1*C*). Thus, myeloid cells are the most frequently represented CD13-expressing stromal cells in these tumors.

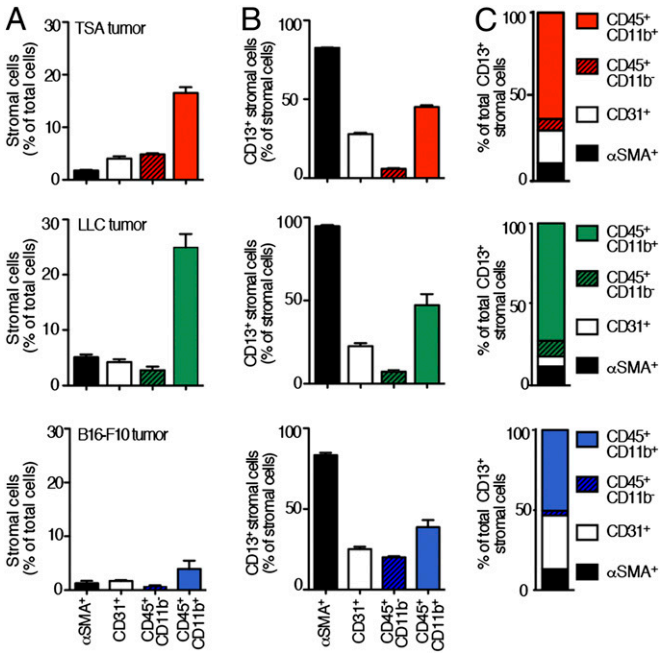

Fig. 1. Characterization of CD13-expressing stromal cells. (*A*) TSA, LLC, and B16-F10 tumor cells (shown and labeled in the vertically positioned graphs) were analyzed by FACS for expression of several cell type-specific markers: αSMA for pericytes/CAFs, CD31 (endothelial cells), and CD45 (immune cells), separated into $CD11b^-$ and $CD11b^+$ groups to distinguish nonmyeloid and myeloid cells. Pericytes and endothelial, myeloid, and nonmyeloid stromal cells are represented as percentage of total tumor cells. Means ± SEM are shown. (*B*) CD13-expressing cells in the three tumor cell types represented as a percentage of each stromal cell component. Means ± SEM are shown. (*C*) Distribution of CD13-expressing cells among stromal cells in the three tumor cell types. Means ± SEM are shown. In each case, three to five tumors per experiment were analyzed, and each experiment was performed at least three times. Data from one representative experiment are shown.

Experimental Generation of CD13 WT and KO Bone Marrow-Transplanted Mouse Models. To study the contribution of CD13-expressing stromal cells to tumor growth and potentially to angiogenesis, we developed bone marrow transplant (BMT) mouse models with CD13 WT and KO mice. We transplanted lethally irradiated mice of both genotypes with total nucleated bone marrow cells obtained from WT or KO mice to produce: (*i*) WT^{wt} mice (CD13 WT mice transplanted with bone marrow cells derived from CD13 WT mice); (*ii*) WT^{ko} mice (CD13 WT mice transplanted with bone marrow cells derived from CD13 KO mice); (*iii*) KO^{wt} mice (CD13 KO mice transplanted with bone marrow cells derived from CD13 WT mice); and (*iv*) KO^{ko} mice (CD13 KO mice transplanted with bone marrow cells derived from CD13 KO mice; Fig. S1*A*). These models were designed to evaluate the relative contribution of $CD13^+$ BMDCs versus other stromal components to tumor growth and angiogenesis (Fig. S2).

Four weeks later, mice were genotyped by PCR (for both DNA extracted from nucleated blood cells and from tail tips), and successful engraftment of either WT- or KO-BMDCs was evaluated and confirmed (Fig. S1*B*). Hematological parameters (i.e., red and white blood cells, hemoglobin, and hematocrit) from the sets of mice analyzed were similar, indicating that bone marrow reconstitution did not alter the complete blood count composition (Fig. S1*C*). Long-term bone marrow reconstitution (demonstrated by H&E staining of postmortem femur sections) showed no detectable differences between WT^{wt}, KO^{ko}, WT^{ko}, or KO^{wt} mice (Fig. S1*D*). Finally, the levels of interleukin-2, tumor necrosis factor-α, and IFN-γ released by phorbol-12-myristate-13-acetate/ionomycin-stimulated lymphocytes ($CD45^+CD3^+$) and myeloid cells ($CD45^+CD11b^+$) obtained from WT^{wt}, KO^{ko}, WT^{ko}, or KO^{wt} mice were similar, suggesting that the cells obtained from the various reconstituted mice are also functionally similar (Fig. S1*E*).

In summary, transplanted mice recovered from the BMT and did not show hematological or functional abnormalities.

$CD13^+$ BMDCs Affect Experimental Tumors, Angiogenesis, and Metastasis. We next studied the role of CD13-expressing stromal cells in tumor development. After recovery, BMT mice were administered s.c. with LLC, B16-F10, or TSA tumor cells. Tumor growth in LLC and B16-F10 models was significantly impaired in KO^{ko} mice (displaying no CD13-expressing stromal component), compared with WT^{wt} mice, as also previously shown with LLC and B16-F10 transplanted tumors (12); tumor growth was severely impaired in the TSA tumor model as well. The growth of LLC, TSA, or B16-F10 tumors was also significantly reduced in WT^{ko} mice, which specifically lack only $CD13^+$ BMDCs (Fig. 2 *A* and *B*). Consistent with these observations, tumor growth was restored in both LLC- and TSA-bearing KO^{wt} mice, which express CD13 only on BMDCs but not on pericytes, endothelial cells, or CAFs (Fig. 2 *A* and *B*). Only B16-F10 tumor growth remained unrescued in the presence of $CD13^+$ BMDCs (Fig. 2 *A* and *B*). We also analyzed the role of $CD13^+$ BMDCs on tumor growth at secondary sites by tail vein injection of tumor cells in BMT mice. Similar to the results for primary tumor growth, the absence specifically of $CD13^+$ BMDCs clearly reduced the formation of lung colonies (Fig. 2*C*). We conclude that $CD13^+$ BMDCs are an important stromal component for growth at both the primary tumor site and secondary experimental metastasis sites.

$CD13^+$ BMDCs Affect Blood Vessel Development in Tumors. To understand how $CD13^+$ BMDCs regulate tumor growth, we analyzed angiogenesis by quantification of CD31 (endothelial cells) and NG2 chondroitin sulfate proteoglycan (NG2, pericytes) immunoreactive blood vessels in LLC, TSA, and B16-F10 tumor sections obtained from WT^{wt}, KO^{ko}, WT^{ko}, and KO^{wt} tumor-bearing mice. Tumors from mice specifically lacking $CD13^+$ BMDCs (i.e., WT^{ko} and KO^{ko}) exhibited lower blood vessel

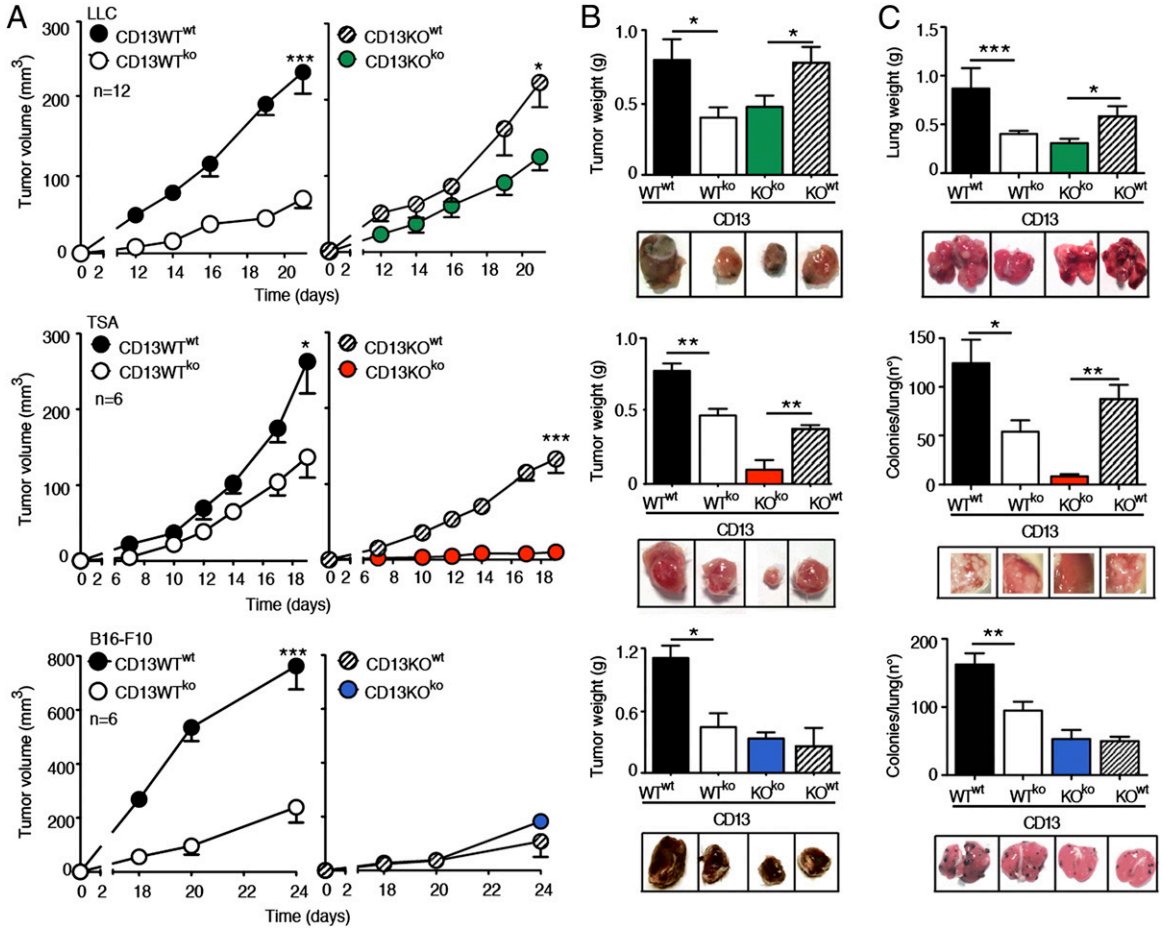

Fig. 2. Experimental tumor growth in BMT mice. (*A* and *B*) LLC, TSA, and B16-F10 tumor growth (mean ± SEM), tumor weight (mean ± SEM), and representative photographs of tumors recovered from BMT mice administered s.c. with tumor cells. (*C*) Lung weight (LLC) or number of lung colonies (TSA, B16-F10) (mean ± SEM) and representative photographs of lungs recovered from BMT mice administered with tumor cells i.v. $*P < 0.05$; $**P < 0.01$; $***P < 0.001$ by two-tailed Student *t* test.

densities (Fig. 3 *A* and *C* and Fig. S3) and lesser coverage with NG2-immunoreactive pericytes (Fig. 3 *B* and *C* and Fig. S3), in comparison with tumors from WT^{wt} mice. Notably, transplantation of $CD13^+$ BMDCs into CD13 KO mice (KO^{wt}) increased the number of blood vessels in LLC- and TSA-derived tumors and blood vessel coverage with NG2-immunoreactive pericytes in comparison with tumors from KO^{ko} mice (Fig. 3 and Fig. S3*A*). Similar to the effect on tumor growth, no rescue was observed in B16-F10–bearing KO^{wt} mice (Fig. S3*B*). Taken together, these results establish that $CD13^+$ BMDCs represent a subset of immune cells whose absence impairs tumor-associated angiogenesis.

$CD13^+$ BMDCs and Angiogenic Blood Vessels Express Different CD13 Isoforms. CD13 has multiple isoforms, and the isoform found on angiogenic blood vessels is recognized specifically by the Asn-Gly-Arg (NGR) (single-letter amino acid code) motif (24). To determine whether the same isoform was also expressed on $CD13^+$ BMDCs, we performed subtractive cell-binding assays with a bacteriophage (phage) clone displaying an NGR motif (NGR-targeted phage) through the biopanning and rapid analysis of selective interactive ligands methodology (25). Tumor-associated BMDCs with and without CD13 expression ($CD45^+CD13^+$ and $CD45^+CD13^-$, respectively) and angiogenic endothelial cells with and without CD13 expression ($CD31^+CD13^+$ and $CD31^+CD13^-$, respectively) were isolated by FACS from TSA-derived tumors and incubated with NGR-targeted phage or untargeted control phage. Only CD13-expressing endothelial cells specifically bound NGR-targeted phage (Fig. S4). These results indicate that BMDCs express an isoform of CD13 different from that displayed by angiogenic endothelial cells.

$CD13^+$ Myeloid Cells Regulate Angiogenesis. Several subsets of BMDCs are well-established contributors to tumor angiogenesis (3, 5). Given that our BMT-based experimental models do not address the contribution of specific subpopulations of BMDCs, we directly analyzed the effect of isolated subsets of $CD13^+$ BMDCs on tumor blood vessel development. $CD45^+CD11b^+CD13^+$, $CD45^+CD11b^+CD13^-$, or $CD45^+CD11b^-CD13^+$ (identified as $CD11b^+CD13^+$ myeloid cells, $CD11b^+CD13^-$ myeloid cells, and $CD11b^-CD13^+$ nonmyeloid cells, respectively) were sorted by FACS from TSA-derived tumors grown in WT mice and coadministered with TSA cells into CD13 KO mice (3×10^4 and 4×10^5 cells, respectively). Sorted cells were also administered directly into the tumors at days 5 and 9 posttumor challenge, and tumor angiogenesis was quantified by immunofluorescence on day 12. Administration of $CD11b^+CD13^+$ myeloid cells rescued angiogenesis, as evaluated by quantification of the number of endothelial cell-containing ($CD31^+$) blood vessels, and markedly restored $NG2^+$ pericyte coverage. The other cell populations did not rescue angiogenesis and pericyte coverage (Fig. 4*A*). Therefore, $CD11b^+CD13^+$ myeloid cells can selectively promote angiogenesis in vivo. To assess whether $CD11b^+CD13^+$ myeloid cells can regulate angiogenesis by affecting endothelial cell migration and organization, we incubated the sorted cells with carboxyfluorescein succinimidyl

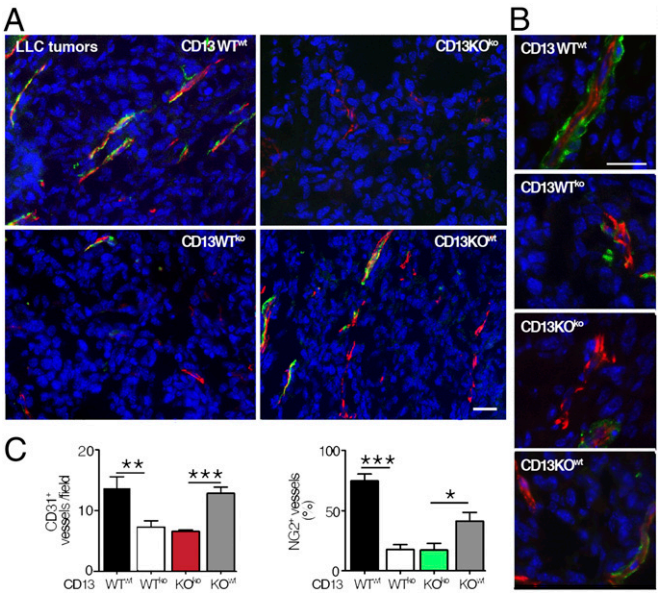

Fig. 3. Evaluation of tumor angiogenesis in LLC tumor-bearing BMT mice. (*A*) Immunohistochemical detection of CD31 (endothelial cells, red) and NG2 (pericytes, green) in LLC tumors recovered from tumor-bearing BMT mice. DAPI, blue. (*B*) Higher magnification of $NG2^+$ and $CD31^+$ blood vessels is shown. (*C*) The number of $CD31^+$ blood vessels per field and the number of $NG2^+$ blood vessels (mean ± SEM) averaged from 10 random fields are shown. Three tumors for each of the BMT group were analyzed. $*P < 0.05$; $**P < 0.01$; $***P < 0.001$ by two-tailed Student *t* test. (Scale bar, 20 μm.)

ester (CFSE)-labeled human dermal microvascular endothelial cells (HDMECs) and analyzed the formation of endothelial tubes after 8 h ("tube-formation" assay). In parallel, we cocultured sorted cells with scratched CFSE-labeled HDMEC monolayers and monitored "wound" closure for 3 d ("wound-healing" assay). No effects were observed in either assay (Fig. 4*B* and Fig. S5). These data suggest that $CD11b^+CD13^+$ myeloid cells do not inhibit angiogenesis in tumors by directly affecting endothelial cell migration and organization and more likely affect the complex interplay between pericytes and endothelial cells within the tumor microenvironment.

$CD13^+$ Myeloid Cells Produce Soluble Angiogenic Factors. To assess whether $CD11b^+CD13^+$ myeloid cells could affect angiogenesis by producing soluble proangiogenic factors, we sorted $CD11b^+CD13^+$, $CD11b^+CD13^-$, and $CD11b^-CD13^+$ from LLC tumors and cultured them in vitro for 5 d. Then, we analyzed the presence of soluble pro-/antiangiogenic factors in their supernatants with the Mouse Angiogenesis Array Kit (R&D). The results showed that (*i*) $CD11b^+CD13^+$ cells secreted matrix metalloproteinase (MMP)-9 and osteopontin (OPN); (*ii*) $CD11b^+CD13^-$ produced OPN, CXCL16, and CXCL4 (a potent inhibitor of angiogenesis); and (*iii*) $CD11b^-CD13^+$ secreted OPN and stromal cell-derived factor-1 (Fig. 4*C*). Thus, $CD11b^+CD13^+$ could selectively release MMP-9, a protease known to play a role in angiogenesis (26).

A lysate of $CD11b^+CD13^+$ myeloid cells was then analyzed using the same angiogenesis array. Besides confirming the production of osteopontin and MMP-9 by $CD11b^+CD13^+$ cells, this assay could also detect the production of monocyte chemoattractant protein (MCP)-1 (Fig. S6*A*). Notably, both MCP-1 and MMP-9 are known to regulate vascular architecture by promoting pericyte recruitment (26, 27).

Finally, we analyzed the release of angiogenic factors by pericytes alone or cocultured with sorted BMDCs. Although various factors were released by these cells, no significant changes were induced by BMDCs in this experimental system (Fig. S6*B*).

Collectively, these data indicate that $CD11b^+CD13^+$ myeloid cells secrete proteins known to affect pericyte biology and angiogenesis.

$CD13^+$ Myeloid Cells Specifically Localize Within Tumors and Macrophages Are the Most Represented $CD13^+$ Population. To investigate the location of $CD11b^+CD13^+$ myeloid cells, we performed a biodistribution study in LLC, B16-F10, and TSA tumor-bearing mice. Single-cell suspensions obtained from blood, bone marrow, brain, spleen, liver, lung, kidney, and tumor were analyzed by FACS. $CD11b^+CD13^+$ myeloid cells were found only in tumors, where they represented 10.5%, 2.7%, and 5.11% of LLC, B16-F10, and TSA tumor cells, respectively (Fig. S7 *A* and *B*). Finally, we analyzed the percentage of $CD13^+$ cells in different tumor-infiltrating myeloid and nonmyeloid cell populations. CD13-expressing cells were identified as monocytes ($CD45^+CD11b^+Ly6G^-Ly6C^+CD13^+$), macrophages ($CD45^+CD11b^+F4/80^+CD13^+$), granulocytes ($CD45^+CD11b^+Ly6G^+Ly6C^+CD13^+$), dendritic cells ($CD45^+CD11c^+CD13^+$), CD4 T lymphocytes ($CD45^+CD4^+CD13^+$), and CD8 T lymphocytes ($CD45^+CD8^+CD13^+$). Although CD13 was expressed by monocytes and granulocytes, macrophages were the most represented population, comprising 18% of the BMDCs (Fig. S7*C*). Fewer $CD13^+$ dendritic cells and CD4 T lymphocytes, and no CD8 T lymphocytes, were identified.

Discussion

In this report, we provide evidence that $CD13^+$ myeloid BMDCs represent a population of proangiogenic immune cells implicated in tumor-associated blood vessel formation. We also show that CD13, a membrane-bound protease, has a central role in their activity. To dissect the relative contributions of different $CD13^+$ cells of the tumor microenvironment, we have generated syngeneic tumor models based on CD13 WT and KO mice transplanted with CD13-positive or -negative bone marrow recovered from the same mice to obtain different combinations called WT^{wt}, WT^{ko} KO^{wt}, and KO^{ko} (see Fig. S2 for a schematic representation of the experimental system). The growth of different tumor cells (namely B16-F10 melanoma, TSA adenocarcinoma, and LLC lung carcinoma) in these mice was subsequently investigated in vivo. The results showed that growth of all these tumors and angiogenesis within them is severely impaired in mice lacking $CD13^+$ BMDCs (KO^{ko} and WT^{ko}), and this impairment is associated with a reduction in both vascular density and pericyte coverage in tumor tissues. Restoring $CD13^+$ BMDCs in CD13-negative mice (KO^{wt}) rescued tumor growth and angiogenesis in the TSA and LLC models but not in the B16-F10 model.

These results clearly indicate that $CD13^+$ BMDCs have a role in tumor-related angiogenesis and blood vessel stabilization. The different results, in quantitative terms, obtained with different tumor models (particularly in the "rescue" experiment) suggest that tumor cells have a role in the cross-talk between $CD13^+$ BMDCs and the tumor microenvironment during angiogenesis.

The role of BMDCs in tumor angiogenesis has been increasingly investigated in recent years. Proangiogenic BMDCs include different myeloid subsets: granulocytes, monocytes/macrophages, dendritic cells, mast cells, myeloid suppressor cells, and other populations (e.g., progenitor cells) (3). Monocytes (circulating and resident) can differentiate into various functional subpopulations of TAMs, whose phenotypes are regulated by the milieu of cytokines present within the tumor microenvironment (3). Although the developmental relationships between monocyte/macrophages subsets are still poorly defined, monocytes have been shown to produce at least two distinct macrophage populations: the $CD11c^+$ TAMs and TEMs (28). Both populations can support angiogenesis by producing different proangiogenic cytokines, such as

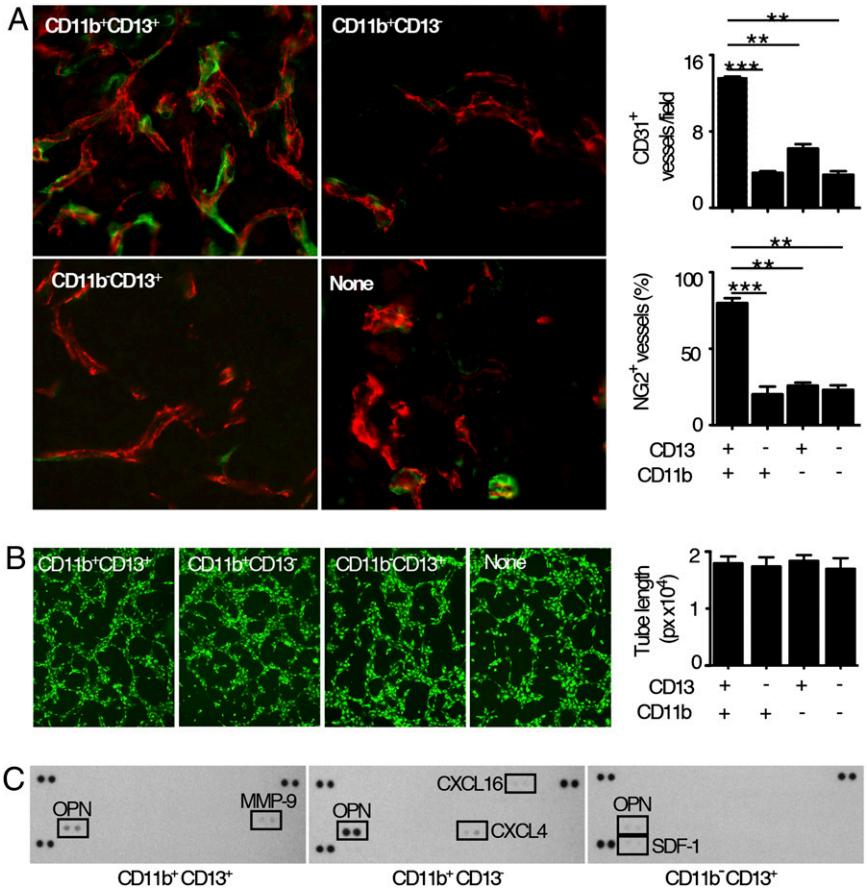

Fig. 4. Effect of sorted BMDCs on angiogenesis. (*A*) Immunohistochemical detection of CD31 (endothelial cells, red) and NG2 (pericytes, green) in TSA tumors. The number of $CD31^+$ blood vessels per field and the number of $NG2^+$ blood vessels (mean ± SE) averaged from 10 random fields are shown. Three tumors per each group were analyzed. (*B*) In vitro tube-formation assay. CFSE-labeled HDMECs were incubated with sorted CD13-expressing myeloid cells ($CD11b^+CD13^+$), CD13-expressing nonmyeloid immune cells ($CD11b^-CD13^+$), and CD13-negative myeloid cells ($CD11b^+CD13^-$). Images were taken after 8 h, and tube length was analyzed by WimTube software. Representative images are shown (mean ± SEM). Each experiment was performed three times in quadruplicate. Data from one representative experiment are shown. (*C*) Analysis of angiogenic proteins secreted by $CD11b^+CD13^+$, $CD11b^+CD13^-$ and $CD11b^-CD13^+$ cells. Cells (1.5×10^5) were isolated by FACS from LLC tumors grown in CD13 WT mice and cultured for 5 d in DMEM, 2% FBS. The supernatants were then analyzed with the Mouse Angiogenesis Antibody Array Kit (R&D). Immunoreactive spots (in duplicate) are shown. Immunoreactive control spots are also shown at the corners. $^{**}P < 0.01$; $^{***}P < 0.001$ by two-tailed Student *t* test. (Scale bar, 20 μm.)

basic fibroblast growth factor, vascular endothelial growth factor (VEGF), and MMP-9 (7, 29, 30). The depletion of proangiogenic macrophages (e.g., induced by ablation or pharmacological neutralization or suppression of their recruitment) can inhibit tumor growth by preventing production of proangiogenic, tumor-promoting, and immunosuppressive factors (3). Granulocytes, mast cells, and myeloid-derived suppressor cells also can play a role in angiogenesis by producing proangiogenic factors, such as VEGF-A and MMP-9 (30). Neutrophils, in particular, together with monocytes and macrophages, were identified as the most important producers of MMP-9, a protease that affects the interactions of VEGF with VEGFR2 by promoting MMP-9 bioavailability, thereby inducing angiogenesis (30). Our results show that $CD13^+$ myeloid BMDCs cells, but not $CD13^-$ myeloid cells or $CD13^+$ nonmyeloid immune cells, can rescue tumor angiogenesis in vivo when administered to KO mice. However, none of these cell populations could promote capillary-like tube formation by endothelial cells in vitro. This result suggests that interaction of $CD13^+$ myeloid BMDCs with other cells of the tumor microenvironment is necessary for angiogenesis stimulation. Interestingly, we found that $CD13^+$ myeloid cells can specifically produce detectable levels of MCP-1 and MMP-9. Given that both MMP-9 and MCP-1 are key factors for pericyte recruitment, a cell type known to consolidate vascular architecture and prevent blood vessel regression (26, 27, 31), this finding suggests that $CD13^+$ myeloid BMDCs cells can promote angiogenesis and vascular maturation by regulating pericyte recruitment.

The identification of $CD13^+$ myeloid BMDCs as participants in tumor angiogenesis could have important implications for development of therapeutic strategies against cancer. First, the observation that these cells are localized almost exclusively within tumors makes them an attractive potential deliverer of therapeutics to the tumor microenvironment. Second, $CD13^+$ myeloid BMDCs may represent a target for antiangiogenic therapeutics. Given the crucial role of CD13 in the activity of these cells, compounds inhibiting this ectoenzyme could have therapeutic benefit. In addition, CD13 ligands could be exploited for delivering drugs to these cells within the tumor microenvironment. CD13 peptide ligands containing the CNGRC motif, identified by phage display technology, have previously been exploited to deliver cytokines, cytotoxins, apoptotic peptides, and even liposomes to tumor blood vessels (20, 32–34). Unfortunately, our results of CNGRC peptide-binding experiments show that $CD13^+$ BMDCs are not targeted by this peptide, likely owing to expression of different CD13 isoforms in $CD13^+$ BMDCs and endothelial cells. Indeed, it has been demonstrated previously by histochemical analysis that differentially immunoreactive forms of CD13 are expressed in tumor-associated blood vessels, myeloid cells, and

epithelia (24). The structural determinants of this selectivity are still unknown. It has been postulated that the use of alternative glycosylation sites or changes in the composition of oligosaccharides may mask antibody or peptide-binding sites (35). Peptide-binding selectivity might also be related to differential formation of quaternary complexes with other proteins in different tissues. Further studies are necessary to clarify this issue. In any case, it should be possible, in principle, to develop other peptides or antibody ligand selective for the $CD13^+$ form expressed by BMDCs or for other markers of these proangiogenic cells, as accomplished previously with the endothelial cells. A valid and realistic approach is to exploit phage display libraries to identify ligands and/or to fingerprint the BMDCs surface to identify receptors expressed as these cells home to tumors.

In summary, our results suggest that $CD13^+$ myeloid BMDCs are the most represented CD13-expressing cells in the tumor microenvironment and have mechanistic roles in tumor growth and metastasis by affecting pericyte biology and angiogenesis.

Materials and Methods

Cell Lines, Drugs, Antibodies, and Reagents. We obtained mouse B16-F10 cells and LLC cells from the American Type Culture Collection and HDMECs and human pericytes from PromoCell. TSA mammary adenocarcinoma cells were a gift from Giulia Casorati (San Raffaele Scientific Institute, Milan). Rabbit polyclonal anti-cleaved caspase 3, anti-NG2 chondroitin sulfate proteoglycan, and anti-αSMA were purchased from Cell Signaling, Chemicon, and Abcam, respectively. Rat monoclonal anti-CD31 was from Abcam, and CFSE was from Sigma.

Generation of Bone Marrow-Transplanted Mice. All of the animal studies were approved through the Institutional Animal Care and Use Committee of the University of Texas M. D. Anderson Cancer Center. CD13 WT and KO BALB/c and C57BL/6 mice were generated as described (12, 22). Recipient 8- to 12-wk-old CD13 WT and KO mice were whole body-irradiated in a cobalt irradiator at 12 Gy per mouse (two rounds of radiation at 6 Gy each, with a 2-h recovery interval). Donor CD13 WT and KO mice were killed, and bone marrow cells from femur and tibia were flushed with PBS containing 2% (vol/vol) FBS and washed in PBS. The cells were resuspended in hypotonic solution to lyse red blood cells, and subsequently washed again in PBS. Three hours after the last round of radiation, recipient mice received $5–10 \times 10^6$ total nucleated BMDCs i.v. Following BMT, mice received enrofloxacin (Bayer) in the water for 4 wk. Control mice that were radiated but not transplanted died within 12–14 d.

Tumor and Experimental Metastasis Studies. BMT BALB/c mice received TSA cells (4×10^5) s.c. BMT C57BL/6 received either LLC cells (1×10^6 per mouse) s.c. or B16-F10 cells (5×10^5 per mouse) s.c. Tumor sizes were measured with a caliper until mice were killed. Tumors were collected and immersed in OCT. For experimental metastasis models, BMT BALB/c mice received TSA cells (7×10^4 per mouse) i.v. BMT C57BL/6 mice received either LLC (1.5×10^5 per mouse) i.v. or B16-F10 cells (1.2×10^5 per mouse) i.v. Lungs were removed and weighed, and metastatic lung colonies were counted under a stereomicroscope. For experiments involving coadministration of tumor and sorted cells, we first purified the populations of interest ($CD45^+CD11b^+CD13^+$, $CD45^+CD11b^+CD13^-$, $CD45^+CD11b^-CD13^+$ cells) from TSA-derived tumors recovered from CD13 WT mice by the FACSAria cell sorter as described above. Sorted cells (3×10^4) were coadministered s.c. with TSA cells (4×10^5) to CD13 KO BALB/c mice and then administered intratumor 5 and 10 d, respectively, after tumor implantation.

FACS analyses; in vitro assays on evaluation of bone marrow reconstitution and lymphocyte and myeloid cell function in BMT mice; immunofluorescence of tumor blood vessels; tube-formation, cell-migration, and angiogenic factor measurements; and cell-binding studies are reported in *SI Materials and Methods*.

ACKNOWLEDGMENTS. This work was supported by grants from the National Institutes of Health and National Cancer Institute and by awards from AngelWorks and the Gillson-Longenbaugh Foundation (all to W.A. and R.P.).

1. Kerbel RS (2008) Tumor angiogenesis. *N Engl J Med* 358(19):2039–2049.
2. Ebos JM, Kerbel RS (2011) Antiangiogenic therapy: Impact on invasion, disease progression, and metastasis. *Nat Rev Clin Oncol* 8(4):210–221.
3. Coffelt SB, et al. (2010) Elusive identities and overlapping phenotypes of proangiogenic myeloid cells in tumors. *Am J Pathol* 176(4):1564–1576.
4. Hanahan D, Coussens LM (2012) Accessories to the crime: Functions of cells recruited to the tumor microenvironment. *Cancer Cell* 21(3):309–322.
5. De Palma M, Naldini L (2006) Role of haematopoietic cells and endothelial progenitors in tumour angiogenesis. *Biochim Biophys Acta* 1766(1):159–166.
6. De Palma M, Murdoch C, Venneri MA, Naldini L, Lewis CE (2007) Tie2-expressing monocytes: Regulation of tumor angiogenesis and therapeutic implications. *Trends Immunol* 28(12):519–524.
7. De Palma M, et al. (2005) Tie2 identifies a hematopoietic lineage of proangiogenic monocytes required for tumor vessel formation and a mesenchymal population of pericyte progenitors. *Cancer Cell* 8(3):211–226.
8. Shi Q, et al. (1998) Evidence for circulating bone marrow-derived endothelial cells. *Blood* 92(2):362–367.
9. Lyden D, et al. (2001) Impaired recruitment of bone-marrow-derived endothelial and hematopoietic precursor cells blocks tumor angiogenesis and growth. *Nat Med* 7(11):1194–1201.
10. Nolan DJ, et al. (2007) Bone marrow-derived endothelial progenitor cells are a major determinant of nascent tumor neovascularization. *Genes Dev* 21(12):1546–1558.
11. van Hinsbergh VW, Engelse MA, Quax PH (2006) Pericellular proteases in angiogenesis and vasculogenesis. *Arterioscler Thromb Vasc Biol* 26(4):716–728.
12. Guzman-Rojas L, et al. (2012) Cooperative effects of aminopeptidase N (CD13) expressed by nonmalignant and cancer cells within the tumor microenvironment. *Proc Natl Acad Sci USA* 109(5):1637–1642.
13. Favaloro EJ, et al. (1988) Further characterization of human myeloid antigens (gp160,95; gp150; gp67): Investigation of epitopic heterogeneity and non-haemopoietic distribution using panels of monoclonal antibodies belonging to CD-11b, CD-13 and CD-33. *Br J Haematol* 69(2):163–171.
14. Mina-Osorio P (2008) The moonlighting enzyme CD13: Old and new functions to target. *Trends Mol Med* 14(8):361–371.
15. Lai A, Ghaffari A, Li Y, Ghahary A (2011) Paracrine regulation of fibroblast aminopeptidase N/CD13 expression by keratinocyte-releasable stratifin. *J Cell Physiol* 226(12):3114–3120.
16. Amoscato AA, Sramkoski RM, Babcock GF, Alexander JW (1990) Neutral surface aminopeptidase activity of human tumor cell lines. *Biochim Biophys Acta* 1041(3):317–319.
17. Calloni R, Cordero EA, Henriques JA, Bonatto D (2013) Reviewing and updating the major molecular markers for stem cells. *Stem Cells Dev* 22(9):1455–1476.
18. Lai A, Ghaffari A, Ghahary A (2010) Inhibitory effect of anti-aminopeptidase N/CD13 antibodies on fibroblast migration. *Mol Cell Biochem* 343(1-2):191–199.
19. Alliot F, Rutin J, Leenen PJ, Pessac B (1999) Pericytes and periendothelial cells of brain parenchyma vessels co-express aminopeptidase N, aminopeptidase A, and nestin. *J Neurosci Res* 58(3):367–378.
20. Arap W, Pasqualini R, Ruoslahti E (1998) Cancer treatment by targeted drug delivery to tumor vasculature in a mouse model. *Science* 279(5349):377–380.
21. Pasqualini R, et al. (2000) Aminopeptidase N is a receptor for tumor-homing peptides and a target for inhibiting angiogenesis. *Cancer Res* 60(3):722–727.
22. Rangel R, et al. (2007) Impaired angiogenesis in aminopeptidase N-null mice. *Proc Natl Acad Sci USA* 104(11):4588–4593.
23. Sugimoto H, Mundel TM, Kieran MW, Kalluri R (2006) Identification of fibroblast heterogeneity in the tumor microenvironment. *Cancer Biol Ther* 5(12):1640–1646.
24. Curnis F, et al. (2002) Differential binding of drugs containing the NGR motif to CD13 isoforms in tumor vessels, epithelia, and myeloid cells. *Cancer Res* 62(3):867–874.
25. Giordano RJ, Cardó-Vila M, Lahdenranta J, Pasqualini R, Arap W (2001) Biopanning and rapid analysis of selective interactive ligands. *Nat Med* 7(11):1249–1253.
26. Chantrain CF, et al. (2004) Stromal matrix metalloproteinase-9 regulates the vascular architecture in neuroblastoma by promoting pericyte recruitment. *Cancer Res* 64(5):1675–1686.
27. Ma J, Wang Q, Fei T, Han JD, Chen YG (2007) MCP-1 mediates TGF-beta-induced angiogenesis by stimulating vascular smooth muscle cell migration. *Blood* 109(3):987–994.
28. Pucci F, et al. (2009) A distinguishing gene signature shared by tumor-infiltrating Tie2-expressing monocytes, blood "resident" monocytes, and embryonic macrophages suggests common functions and developmental relationships. *Blood* 114(4):901–914.
29. Mantovani A, Sozzani S, Locati M, Allavena P, Sica A (2002) Macrophage polarization: Tumor-associated macrophages as a paradigm for polarized M2 mononuclear phagocytes. *Trends Immunol* 23(11):549–555.
30. Nozawa H, Chiu C, Hanahan D (2006) Infiltrating neutrophils mediate the initial angiogenic switch in a mouse model of multistage carcinogenesis. *Proc Natl Acad Sci USA* 103(33):12493–12498.
31. Salcedo R, et al. (2000) Human endothelial cells express CCR2 and respond to MCP-1: Direct role of MCP-1 in angiogenesis and tumor progression. *Blood* 96(1):34–40.
32. Ellerby HM, et al. (1999) Anti-cancer activity of targeted pro-apoptotic peptides. *Nat Med* 5(9):1032–1038.
33. Curnis F, et al. (2000) Enhancement of tumor necrosis factor alpha antitumor immunotherapeutic properties by targeted delivery to aminopeptidase N (CD13). *Nat Biotechnol* 18(11):1185–1190.
34. Pastorino F, et al. (2006) Targeting liposomal chemotherapy via both tumor cell-specific and tumor vasculature-specific ligands potentiates therapeutic efficacy. *Cancer Res* 66(20):10073–10082.
35. Corti A, Curnis F, Arap W, Pasqualini R (2008) The neovasculature homing motif NGR: More than meets the eye. *Blood* 112(7):2628–2635.